Research Square

Preprints are preliminary reports that have not undergone peer review.
They should not be considered conclusive, used to inform clinical practice,
or referenced by the media as validated information.

Discovery of multitargeting inhibitors for the treatment of COVID-19: An in- silico studies

ASO HAMEED HASAN (aso.hameed@garmian.edu.krd)
UTM Skudai: Universiti Teknologi Malaysia https://orcid.org/0000-0002-8375-1664
Narmin Hamaamin Hussen
University of Sulaimani
Sonam Shakya
Aligarh Muslim University
Joazaizulfazli Jamalis
UTM Skudai: Universiti Teknologi Malaysia
Mohammad Rizki Fadhil Pratama
Muhammadiyah University of Palangkaraya: Universitas Muhammadiyah Palangkaraya
Subhash Chander
Amity University Jaipur: Amity University - Jaipur Campus
Harsha Kharkwal
Amity University Jaipur: Amity University - Jaipur Campus
Sankaranarayanan Murugesan
Birla Institute of Technology & Science Pilani

Research Article

Keywords: COVID-19, antiviral compounds, molecular docking, molecular dynamics, ADMET

Posted Date: April 11th, 2022

DOI: https://doi.org/10.21203/rs.3.rs-1503192/v1

License: This work is licensed under a Creative Commons Attribution 4.0 International License. Read Full License

Abstract

Coronavirus disease-2019 (COVID-19), a global pandemic has currently infected more than 247 million people around the world. Nowadays, several receptors of COVID-19 have been reported, and few of them are explored for drug discovery. New mutant strains of COVID-19 are emerging since the first outbreak of disease and causing significant morbidity and mortality across the world. Although, few of drugs were approved for an emergency uses, however, promising drug with well proven clinical efficacy is yet to be discovered. Hence, researchers are continuously attempting for search of potential drug candidates targeting the well-established enzymatic targets of the virus. The present study is aiming to discover the antiviral compounds as potential inhibitors against the five targets in various stages of the SARS-CoV-2 life cycle, i.e., virus attachments (ACE2 and TMPRSS2), viral replication and transcription (M^{pro}, PL^{pro} and RdRp), using the most reliable molecular docking and molecular dynamics method. The ADMET study was then carried out to determine the pharmacokinetics and toxicity of several compounds with the best docking results. To provide a more effective mechanism for demonstrating protein-ligand interactions, molecular docking data were subjected to a molecular dynamic (MD) simulation at 300K for 100 ns. In terms of structural stability, structure compactness, solvent accessible surface area, residue flexibility, and hydrogen bond interactions, the dynamic features of complexes have been compared.

Introduction

Since two years, the first case of SARS-CoV-2 was reported in Wuhan, China, various variations of concern (VOC) have emerged around the worldwide, with some variants appearing to pose a higher risk to public health resulting in increased transmissibility or cause more severe disease [1–3]. According to latest reports by the World Health Organization (WHO), as of 04:33 pm CET, 8 February 2022, total cases of COVID-19 worldwide were over 396, 558, 014 accounting for more than 5, 745, 02 deaths [4]. Several spikes were observed throughout the world since the outbreak of disease. Although several drugs were provisionally approved by the different regulatory bodies from ranging from small drug molecules to monoclonal antibodies across the world for the treatment of COVID-19, but none of them unanimously proven promising active in the clinical use [5].

To date, potential strategies to control the outbreaks of coronavirus is vaccination [6]. Subsequently, in less than a year, numerous vaccines against the novel coronavirus disease (COVID-19) were developed, giving us all hope of being free from the widespread disease [7]. The approved COVID-19 vaccines are proposed to protect against the disease by developing active immunity, decreased risk of developing the illness and COVID-19 associated complications. The focus has now turned to ensuring widespread vaccine coverage as soon as possible around the world [8, 9]. Although, the use of vaccines to prevent the pandemic is still fraught with difficulties. After few months fall, sharp rise in the COVID-19 cases in the December 2021 and starting of January 2022 9 even among the full vaccinated population across the world, particularly, USA, Europe and Asian countries, again raise concern about the long-term efficacy of available vaccines [2].

Vaccine availability is another major concern. Globally, around 951.26 million people had been vaccinated as of February 7, 2022. [10]. In addition, the main reasons for the low vaccination rate around the world is a shortage of vaccinations, particularly in developing countries. Another explanation could be people's unwillingness to be vaccinated. [7].

Unfortunately, the numbers of people affected by COVID-19 are expected to be repeatedly fluctuate over the coming months [11]. As indicated, these viruses do not only affect the unvaccinated; there have been reports of breakthrough infections in people who have been fully vaccinated. [12]. However, it is unlikely that any of the available vaccines will be 100% effective at stopping transmission or infection to other [13]. Many clinical evidence indicates that the overall infection risk, from severity to mortality can be tamed down effectively with vaccines, being immunized can also make people develop slightly different symptoms than unvaccinated ones [14, 15]. In general, vaccines are effective for prophylactic use i.e effective when administered prior to infection (prophylactic), but potent antiviral agents are required to treat people who already have COVID-19 infection [16]. Currently, there are several repurposed drugs such as, hydroxychloroquine/azithromycin, favipiravir, hydroxychloroquine, lopinavir/ ritonavir, remdesivir, arbidol, and lopinavir/ ritonavir combined with interferon beta [17].

In the beginning of November, two new antiviral drugs were reported to reduce death as well as hospitalization numbers among patients who were treated early after their initial infection in clinical studies. The United Kingdom became the first country to approve molnupiravir on 4 November, which was developed by Merck and Ridgeback Biotherapeutics. The approval comes just over a month after the companies declared that the antiviral medicine, to be marketed by Lagevrio, reduce the risk of hospitalization cases with

mild or moderate COVID-19 by 50%. Furthermore, in non-hospitalized adult patients with mild to moderate COVID-19 who were treated within five days of symptom onset, molnupiravir reduced the risk of death or hospitalization by almost half. Meantime, a day after the UK approval, Pfizer, based in New York City, that its antiviral medicine Paxlovid had decreased 89 percent of hospitalizations. On 16 November, the FDA has been formally allowed Pfizer for emergency use authorisation of the oral pill [18]. Despite above mentioned, there is still an urgently need to look for specific antiviral drugs and additional clinical trials are needed to investigate their inhibitory mechanisms, efficacy, and safety in the treatment of coronavirus infection. [19–21].

Many researchers have focused on some targets in order to discover and develop potential antivirals by blocking major steps in the life cycle of COVID-19 [22]. Targeting the lifecycle steps of SARS-CoV-2, including virus attachment, viral replication, transcription, as well as virus assembly and release, provides possible targets for clinical intervention [23]. The cell entry of SAR-COV-2 depends on the binding of the viral spike (S) proteins to human cellular receptors and on the S protein priming by host cell proteases [24, 25]. The viral S protein is cleaved into S1 and S2, the S1 which interacts with angiotensin-converting enzyme 2 (ACE2) and S2 which is again split and stimulated by transmembrane protease serine 2 (TMPRSS2). Therefore, the fusion of viral-host membrane will be occur resulted of these actions. these high-affinity interactions are required for viral entry, they are prime targets in COVID-19 treatment. Chloroquine has previously been reported to inhibit the virus-receptor interaction in SARS-CoV infection by interfering with the terminal glycosylation of ACE2. Furthermore, both Camostat and Nafamostat are TMPRSS2 inhibitors that have been found to be effective against MERS-CoV in clinical trials [26–33].

Subsequently, the virus gets uncoated after entering the host body, and begins genome replication, which is followed by translation at the cytoplasmic membrane, which is assisted by a coordinated RNA synthesis process mediated by a protein complex encoded by the 20kb replicase gene [34]. In the cell, novel SARS-CoV-2-specifc antiviral drugs can target the virus' main protease (M^{pro}), also known as a chymotrypsin-like cysteine protease, $3CL^{pro}$) and the papain-like protease (PL^{pro}) because of its importance in the processing of polyproteins translated from the SARS-CoV-2 RNA-dependent RNA polymerase (RdRp) or viral RNA which is needed for viral genome replication and transcription of viral genes [35–41]. Moreover, Drugs that target viral proteins have a significant benefit in that they may have greater specificity against the virus while having less side effects in humans. The COVID-19 M^{pro} and PL^{pro} as an interesting target to safely encounter the viral disease since they are essential for COVID-19 replication, highly conserved across related viruses, and not present in humans [42–44]. The very recently Paxlovid is an antiviral drug developed by Pfizer which acts as an orally active M^{pro} or 3CL protease inhibitor [45]. M^{pro} is known to be inhibited by the fixed-dose combination of Ritonavir and Lopinavir (Kaletra) which is allowed for the treatment of HIV/AIDS. [46]. Unfortunately, the Kaletra has shown to be ineffective in treating SARS-CoV-2 in preliminary clinical trials [47], nevertheless it's currently being tested in combination with other antiviral medications. Moreover, Disulfiram, an alcohol-aversive medication that is available in the clinic, has been found to inhibit PL^{pro} in both SARS-CoV and MERS-CoV [48, 49]. In addition, a number of RdRp inhibitors reported to be ineffective in treating COVID-19 infections were originally developed for different viruses. Remdesivir, an adenosine analog prodrug, was originally designed for the treatment of EBOV and has wide antiviral activity against RNA viruses [50]. Remdesivir therapy in animal models has been positive against infection with MERS-CoV and SARS-CoV [51, 52]. *In vitro* SARS-CoV-2 replication had been inhibited by Remdesivir [53]. Other RdRp inhibitors include favipiravir, ribavirin and molnupiravir [46, 54–56].

The last week of November 2021, WHO designated a new variant B.1.1.529, name it Omicron, and put it under the category of 'variant of concern'. Although sufficient data is not documented about the mortality of the virus but due several mutations and very high transmission rate has been reported [57]. No specific known drugs are available for SARS-CoV-2, there is still an urgently need to look for specific antiviral drugs and the global attention focused on the scientific community for a possible solution [21, 37, 44].

Researchers are adopting experimental and computational methods to find potential medications from the FDA-approved drug library. The computational modeling approaches including, *in silico* ADMET/drugs-likeness prediction, molecular docking and molecular dynamics simulations are adopted mainly to discover potential drug candidates from several databases. These approaches saves time and reduces the cost in the field of drug discovery [58–62]. There are some recent studies suggesting the use of traditional medicines as an adjuvant for the administration of COVID-19, therefore efforts to integrate the use of both western medicines and drugs for designing appropriate therapy strategies are still ongoing [63–65]. Numerous studies well documented that the phytochemicals such as terpenoids, lignans, coumarins, saponins, stilbenes, alkaloids, flavonoids, tannins and steroids play a variety of roles in viruses (hepatitis C virus (HCV), herpes simplex virus (HSV), dengue, chikungunya, influenza, SARS) includes genetic material and destroying nucleocapsid, inhibiting viral entrance and reducing the virus reproduction [66–79].

In this manuscript, 305 phytochemicals from terpenoids, lignans, coumarins, saponins, polyphenols stilbenes, alkaloids, flavonoids, tannins and steroids were selected based on their reported antiviral activities to discover hit compounds for the five protein targeting various stages of the SARS-CoV-2 life cycle, i.e., virus attachments (ACE2 and TMPRSS2), viral replication and transcription (Mpro, PLpro and RdRp). To discover the promising agents against SARS-CoV-2, the selected compounds were evaluated using in silico ADMET and drugs-likeness prediction, molecular docking, and molecular dynamics simulations.

Methodology

Preparation of ligand

The structure data file (SDF) format of each bioactive compounds and drugs were downloaded from NCBI PubChem database (https://pubchem.ncbi.nlm.nih.gov/). All structure data file (SDF) format of each ligand were subjected to energy minimization process utilizing the Merck Molecular Force Field 94 (MMFF94) force field algorithm [80]. The PyRx software was used to save the minimized structures as PDBQT.

Preparation of receptors

The crystal structure of COVID-19 receptors, main protease (PDB ID: 6LU7), Human Angiotensin Converting Enzyme (PDB ID: 1O86), primer RNA (RdRp) (PDB ID: 7BV2), Trans membrane Protease Serine 2 (TMPRSS2) (PDB ID: 7MEQ) and Papain-like protease (PL^{pro}) (PDB ID: 6WX4) were retrieved from the RCSB website (www.rcsb.org). The water molecules, heteroatoms and co-crystallized ligands were removed using Discovery studio 2021 client [81]. The polar hydrogens and Kollman charges were added. Partial charges of the molecule were calculated using Geistenger method. The PDB files were converted into PDBQT file format using Autodock tool [82].

Molecular docking protocol

Molecular docking simulations of the target compounds were investigated by using AutoDock Vina program [83]. The Vina software was run in exhaustiveness = 8. The binding sites was selected based on their co-crystallized ligands with the target proteins. AutoDock Vina affinity scores (in kcal/mol) for all compounds were obtained and ranked using the free energy binding theory. The generated docking poses were graphically analyzed to check the interactions utilizing Using Discovery Studio Visualizer. It was also used to draft 2D and 3D figures of ligand-receptor complex.

In-silico ADMET analysis

The prediction of drug-likeness and ADMET (Absorption, Distribution, Metabolism, Excretion, and Toxicity) properties of the selected compounds was carried out utilizing online servers such as SwissADME, ProTox-II, and pkCSM, as reported in literature [84].

Molecular dynamics (MD) simulation

The best complex (protein-ligand) pose of proteins 1O86 and 6LU7 with ligand obtained from molecular docking was used for MD simulation. The GROMACS version 2019.2 package was utilized to investigate MD simulation analysis with GROMOS96 43a1 force field. Parameter files and topology of the withanolide was generated using the latest CGenFF through CHARMM-GUI [85, 86]. SPC water models that extended 10 Å from the protein were used to solve complex structures in a triclinic box [87]. To mimic the physiological salt concentrations, 55 Na^+ and 42 Cl^- ions (0.15 M salt) for 1O86-withanolide complex (Fig. 1(a)) and 33 Na^+ and 29 Cl^- ions (0.15 M salt) for 6LU7-withanolide-complex (Fig. 1(b)) were added to neutralize the systems. both systems (NPT and NVT equilibration run were subjected to periodic boundary conditions at (300 K and 1.0 bar) for 100 ns simulation time using a Leap-frog MD integrator [88]. Energy minimization using the steepest descent approach with 5000 steps was used to eliminate bad contact inside the system [89]. Hydrogen bonding were examined using the gmx hbond tool. The gmx gyrate and gmx sasa tools were used to calculate the gyration radius and solvent accessible surface area, respectively. Using the gmx rmsf and gmx rms tools, the root mean square fluctuations (RMSF) and root mean square deviation (RMSD) of protein were computed. Trajectory analysis was carried out

using GROMACS analysis tools [90]. Plots were generated by Grace software, and these plots were visualized *via* PyMol/VMD [91, 92]. Simulations were conducted using processor Intel(R) Xeon(R) CPU E5-2680 v4 @ 2.40GHz, 64 bit.

Results And Discussion

Study outline

Initially, 305 alkaloids constituents, coumarins, flavonoids, lignans, phenols, saponins, steroids, stilbenes, tannins and terpenoids obtained from PubChem were used as ligands for the current study. The absorption, distribution, metabolism and excretion (ADME) profiles of the above-mentioned study compounds were evaluated and screened out 195 ligands (**Table S1**) for docking study, based on Lipinski rule of five, where no violations (Molecular mass less than 500 Dalton, High lipophilicity (expressed as LogP less than 5), less than 5 hydrogen bond donors and less than 10 hydrogen bond acceptors. These properties which were followed as strategic process in drug discovery and development has been implemented in the current study [93]. **Fig. 2** shows the workflow of the present study.

Target receptors selection

As stated in the introduction, a full understanding the life cycle mechanism of SARS-CoV-2 is necessary in order to identify druggable targets for the discovery and development of potent coronavirus therapeutics. In the present study, we have used the potential of natural compounds derived from medicinal plants targeting the SARS-CoV-2 can be divided into two categories, with the first group targeting virus-host interactions (ACE2 and TMPRSS2) or inhibiting viral enzymes (M^{pro}, PL^{pro} and RdRp). These targets play a major role in the viral entry, replication / transcription, the many pharmacological target groups that can be addressed by the traditional de novo drug discovery strategy are reflected in genome and protein synthesis. Accordingly, release and assembly inhibitors are less explored steps in drug discovery against COVID-19 [94]. Despite, most of the drugs for 2019-nCoV are registered for control rather than prophylaxis; ACE2, integrin, and S protein targets are importance for drug repurposing or development programs aimed at preventing viral entrance and fusion. Considering the basic goal of all viruses is to transport and replicate their genetic code in competent host cells, inhibiting the M^{pro}, PL^{pro}, angiotensin-converting enzyme 2 (ACE2), TMPRSS2, and RdRp are suggested to be promising targets for anti-2019-nCoV drug discovery of small molecules.

In addition, targeting human proteins is also a strategy to avoid viral scape caused by mutation. Another option is a multi-target strategy that combines the potential antiviral agents that acting on several targets to enhance efficacy and prevent virus resistance [95]. In light of the COVID-19 pandemic's urgency, the repurposing drugs is a better opportunity to develop a timely and effective cure. In fact, some of the pharmaceuticals currently being tested in clinical trials were originally approved for other purposes [96]. However, past and current coronavirus epidemics necessitate our preparedness not only for the immediate situation, but also for the possibility of novel coronaviruses re-emerging in the future. In this regard, finding equivalent medications that work as pancoronavirus antivirals or using a multi-target approach is crucial to minimize any loss of effectiveness due to viral mutation escape.

Molecular Docking Study

Total around 195 compounds were docked against five receptors including, main protease (M^{pro}) (PDB ID: 6LU7), Human Angiotensin Converting Enzyme (PDB ID: 1O86), primer RNA (Rdrp) (PDB ID: 7BV2), Trans membrane Protease Serine 2 (TMPRSS2) (PDB ID: 7MEQ) and Papain-like protease (PL^{pro}) (PDB ID: 6WX4). The docking scores of all the study compounds were between -11.2 and -4.3 kcal/mol (**Table S1**). These compounds were compared with clinical drugs such as ritonavir, lopinavir, hydroxychloroquine, chloroquine, favipiravir, remdesivir, camostat, nafamostat and disulfiram (**Table S2**).

Docking results for main protease showed that 21 compounds showed stronger binding energy in the range of -9.1 and -7.9 kcal/mol as compared to control drugs, ritonavir (-7.1 kcal/mol) and lopinavir (-7.8 kcal/mol). As shown in **Table 1**, main protease amino acid residues MET6, ILE152, ASP153, ARG298, SER301 and GLY302 exhibited hydrogen bond with 3-HDH-withanolide F. Additionally, the alkyl interaction with PRO9 was also observed. These interactions were resulted in the binding energy of − 9.1 kcal/mol. The possible binding modes of 3-HDH-withanolide F at main protease active sites have been shown in **Fig. 3**.

Table 1

Docking scores and interaction modes of top hit selected antiviral compounds with COVID-19 M^{pro} receptor

No.	Compound	Score	Interactions	
		Kcal/mol	H	Hydrophobic
9	3-HDH-withanolide F	-9.1	MET6, ILE152, ASP153, ARG298, SER301, GLY302	Alkyl: PRO9
12	Limonin	-8.7	ARG131, LYS137, LEU287	π-Alkyl: LEU286, LEU287
2	Withanolide	-8.6	LYS137, ASN238, LEU286, LEU287	Alkyl: LEU286
16	(18R)-Withaphysalin F	-8.6	ARG40, TYR54, GLU55, PHE181	
8	Obacunone	-8.6	THR199, GLY275, MET276	π-Alkyl: LEU286
89	Mimulone	-8.5	THR199, ASN238	π-Sigma: LEU272 Alkyl: VAL171, ALA194
1	Withanolide J	-8.4	TYR37, LYS88, TYR101	Alkyl: VAL35, LYS90
79	Inophyllum C	-8.4	GLN110, THR292, PRO293	π-Sigma: ILE249 π-π Stacked: PHE294 π-Alkyl: PRO293
5	Withanolide N	-8.3	MET276, ASN277, GLY278	π-Alkyl: TYR239
78	Inophyllum P	-8.3	ARG131, THR199, ASN238	

On the other hand, ligands were docked at the active site of ACE target, the results demonstrated that 182 ligands could inhibit target receptors with a potential energy from -11.2 to -7.0 kcal/mol which were most potent than hydroxychloroquine (-6.8 kcal/mol) and chloroquine (-6.9 kcal/mol). It was found that withanolide exhibited highest docking score of -11.2 kcal/mol (**Table 2**). As shown in **Fig. 4**, the molecular interactions holding by withanolide in the active site resulted in the formation of five H-bond with amino acid residues namely GLN281, ASN374, GLU376, HIS383 and ASP415. Furthemore, four hydriphobic interactions were observed including two alkyl and π-alkyl interaction with PRO163, VAL380, TRP279 and HIS383 aminoacid residues.

Table 2

Docking scores and interaction modes of top hit selected antiviral compounds with COVID-19 ACE receptor

No.	Compound	Score	Interactions		
		Kcal/mol	H	Hydrophobic	Other
2	Withanolide	-11.2	GLN281, ASN374, GLU376, HIS383, ASP415	Alkyl: PRO163, VAL380, π-Alkyl: TRP279, HIS383	
16	(18R)-Withaphysalin F	-11.2	GLN281, THR282, ALA354, HIS513	Alkyl: ALA354, VAL380, VAL518 π-Alkyl: HIS353, HIS383, HIS387, PHE512, TYR523	
13	Withasomnilide	-11.1	ASN70, ARG124, ALA356, GLU143	Alkyl: LEU139, LEU140, VAL518 π-Alkyl: HIS353, TRP357, HIS387, PHE512, HIS513	
89	Mimulone	-11.0	ALA356, GLU384, HIS387, HIS513	π-π T-shaped: TRP357 π-Alkyl: HIS353, HIS383, PHE457, HIS513, TYR523, PHE527	π-Sigma: PHE457
10	Somniferanolide	-11.0	GLY404, HIS410, GLU411, ARG522	Alkyl: MET223, PRO407, π-Alkyl: TRP357, HIS387	π-Sigma: TRP357, HIS410
12	Limonin	-10.9	HIS353, SER355, TYR394, HIS410,	π-π T-shaped: HIS353	π-Cation: HIS353
1	Withanolide J	-10.8	ARG522, GLU411	Alkyl: VAL351, VAL518 π-Alkyl: HIS353, HIS387, PHE512	π-Sigma: HIS387
9	3-HDH-withanolide F	-10.7	ASN66, GLU411	Alkyl: LEU81, LEU140, VAL518 π-Alkyl: TYR69	
14	7-Deacetylgedunin	-10.7	ALA354, ASP453, LYS454	Alkyl: VAL380 π-Alkyl: VAL379, PHE457	π-Sigma: GLU376 π-Anion: GLU376
6	Withasomniferanolide	-10.6	ASN70, SER355, ALA356, ARG522	π-Alkyl: TRP357, HIS387, HIS410	π-Sigma: TRP357, HIS387

Meanwhile, the minimum binding energies of docked ligands to the RdRp enzyme indicated that 50 of them (-7.2 to -8.2 kcal/mol) could strongly inhibit target protein as compared to the standard drugs, favipiravir and remdesivir with binding energy of -5.8 and -7.1 kcal/mol, respectively. The ligands were ranked according to their protein-ligand binding energies, aurantinidin was found most active compound with binding energy of -8.2 kcal/mol (**Table 3**). The interactions of aurantinidin and COVID-19 RdRp established five hydrogen bonds (ARG553, TRP617, ASP618, TYR619 and ASP760) to the amino acid residues. Moreover, another interaction was also observed with ASP618 and ASP760 residues *via* π-anion interaction type (**Fig. 5**).

Table 3

Docking scores and interaction modes of top hit selected antiviral compounds with COVID-19 RdRp receptor

No.	Compound	Score	Interactions		
		Kcal/mol	H	hydrophobic	Other
28	Aurantinidin	-8.2	ARG553, TRP617, ASP618, TYR619, ASP760		π-Anion: ASP618, ASP760
87	Tomentin A	-8.1	ASP618, ASP623, SER759, ASP760	π-Alkyl: CYS622, ALA688	π-Anion: ASP760
10	Somniferanolide	-8.0	ARG555, THR687, ASN691, ASP760		
31	Europinidin	-7.9	TYR456, ARG555, THR556, SER759	π-Alkyl: ALA688	π-Cation: ARG555 π-Anion: ASP623
91	Scutellarein	-7.8	ASN691	π-Sigma: SER682	π-Cation: ARG555 π-Anion: ASP623
29	Cyanidin	-7.8	ASP452, TYR456, ARG555, THR556		π-Anion: ASP623
31	Herbacetin	-7.7	ASN691, ASP760	π-Alkyl: ALA558 π-Sigma: SER682	π-Cation: ARG555 π-Anion: ASP623
45	Pedalitin	-7.7	ASN691, SER681, SER682	π-Sigma: SER687	π-Cation: ARG555 π-Anion: ASP623
60	Silymarin	-7.7	THR556, THR680, SER682, ASP760		π-Cation: ARG555 π-Anion: ASP623, ASP760
83	Herbacetin	-7.7	ARG555, SER682, SER759		π-Cation: ARG555 π-Anion: ASP623

Trans Membrane Protease Serine 2 (TMPRSS2) receptor have been inhibited by 7 tested compounds, the binding score of these compounds revealed that they are most active as compared to standard drugs camostat (-7.6 kcal/mol) and nafamostat (-7.7 kcal/mol) as shown in **Table 4**. Silibinin with a binding affinity score of -8.4 kcal/mol showed signiifcant inhibitory activity against target receptor. The interactions between silibinin and residues in TMPRSS2 were shown in **Fig. 6**. This compound binds with VAL280, HIS296, THR393 and GLY439 residues of receptor through H-bond. Four amino acid residues VAL278, VAL280, CYS281 and CYS297 were formed π-alkyl interaction type, whereas two alkyl interactions were also established between VAL280 and LEU302 residues and Silibinin.

Table 4

Docking scores and interaction modes of active compounds with COVID-19 TMPRSS2 receptor

No.	Compound	Score	Interactions		
		Kcal/mol	H	hydrophobic	Other
59	Silibinin	-8.4	VAL280, HIS296, THR393, GLY439	π-Alkyl: VAL278, VAL280, CYS281, CYS297 Alkyl: VAL280, LEU302	
60	Silymarin	-8.4	VAL280, HIS279, GLN438, GLY464	π-Sigma: VAL280 Amide-π Stacked: CYS437 π-Alkyl: CYS465	
16	(18R)-Withaphysalin F	-8.4	HIS296, SER441		
87	Tomentin A	-8.0	CYS297, SER436	π-Alkyl: CYS465	π-Cation: HIS296
89	Mimulone	-8.0	VAL280, GLN438, SER441		π-Cation: HIS296 π-Sulfur: CYS465
12	Limonin	-7.9	HIS296, GLY462, GLY464	Amide-π Stacked: TRP461	
2	Withanolide	-7.9	HIS279, THR393	Alkyl: VAL280	

The results of the binding score energy of the same selected compounds for Papain-like protease (PL^{pro}) protein are presented in **Table S1** and 195 compounds were scored higher than disulfiram (-4.1 kcal/mol). Therefore, somniferanolide appeared as the most active inhibitor for target protein. The binding site interaction between Somniferanolide and 6WX4 happens at TYR207 and VAL202 *via* π-alkyl and alkyl, respectively. Furthermore, four H-bonds were also observed between this compound and PL^{pro} residues including ARG166, SER170, GLN174 and GLU203 (**Fig. 7**).

Table 5

Docking scores and interaction modes of top hit selected antiviral compounds with COVID-19 PL^{pro} receptor

No.	Compound	Score	Interactions		
		Kcal/mol	H	hydrophobic	Other
10	Somniferanolide	-8.6	ARG166, SER170, GLN174, GLU203	π-Alkyl: TYR207 Alkyl: VAL202	
16	(18R)-Withaphysalin F	-8.3	GLU161, TYR268	π-Sigma: TYR264	
78	Inophyllum P	-8.2	TRP106, ALA288	π- π Stacked: TRP106 π-Alkyl: LYS105, ALA288	π-Cation: LYS105
1	Withanolide J	-8.2	ARG166, TYR207, LYS232	Alkyl: MET206	
79	Inophyllum C	-8.1	ALA288, LEU289	π- π Stacked: TRP106 π-Alkyl: LYS105, ALA288, LEU289	π-Cation: LYS105
89	Mimulone	-8.1	GLU161, ASP164	π-Sigma: TYR264 π-Alkyl: TYR264 Alkyl: PRO247, PRO248	π-Cation: LYS157
14	Soulattrolide	-8.1	LYS157	π- π Stacked: TYR264 π-Alkyl: PRO248	
77	Inophyllum B	-8.0	ARG166, SER170	π- π Stacked: TYR171 π-Alkyl: VAL202	
16	Absinthin	-8.0	GLU167, TYR264		
6	Withasomniferanolide	-7.9	LYS157, TYR268	Alkyl: LYS157	

Worth mention, among docked compounds, withanolide, (18R)-withaphysalin F, limonin and mimulone showed the highest binding affinity as compared to the selected drugs in this study. Therefore, the stability of withanolide complexes with each M^{pro} and ACE receptors of COVID-19 were further analyzed using MD simulations for 100 ns duration.

In-silico ADMET prediction

In silico ADMET analysis of the target phytochemicals is presented in **Table 6**. The obtained results which were compared with the results as reported in literature [97], as well as referring to Lipinski's rule of five (LRO5) [98]. The first parameter observed was Mol Wt, where all compounds met the LRO5 criteria, which were ≤500 g/mol. Then compounds silibinin and silymarin showed TPSA values of more than 140 A², exceeding the criteria in LRO5 [99]. The number of hydrogen donor and acceptor groups of all compounds meets the LRO5 criteria, with no more than 5 and 10 groups, respectively. One compound exceeded the LRO5 criteria for the Log P value: compound mimulone with Log P of 5.75, although this value was still within the optimal range of Chander et *al* [100, 101]. All compounds showed ideal Log S values, although all of them were not in the optimal range of CaCo2 values. Only withasomnilide compounds were in the range of Log BB values from Chander et *al* [100, 101], although they all met the criteria for the number of Rot below 15. Finally, there are four compounds (3-HDH-withanolide F, somniferanolide, withasomnilide and (18r)-withaphysalin F) which were predicted to have high toxicity with an LD_{50} value of less than 50 mg/kg and were included in class II of the globally harmonized system of classification of labeling of chemicals (fatal if swallowed) [102], although all compounds did not showed potential as mutagens by the Ames test.

Further analysis of the target toxicity of each compound with ProTox-II was presented in **Fig. 8**. Some of the targets observed were potential carcinogenicity (carcino), immunotoxicity (immuno) and cytotoxicity (cyto); disrupting nuclear receptor signaling pathways

on aryl hydrocarbon receptor (nr_ahr), androgen receptor ligand-binding domain (nr_ar_lbd), estrogen receptor alpha (nr_er) and estrogen receptor ligand-binding domain (nr_er_lbd); as well as interference with stress response pathways to mitochondrial membrane potential (sr_mmp) and tumor suppressor p53 (sr_p53). The results obtained were varied, with the most potential toxicity targets shown by aurantinidin with five targets in the probability range between 0.61 to 0.92. On the other hand, two compounds had the least potential toxicity targets (one target): mimulone and somniferanolide. However, the probability of somniferanolide (0.94) was much higher than mimulone (0.67). In addition, the pLD_{50} of somniferanolide (34 mg/kg) also much lesser than mimulone (2000 mg/kg), so the potential for toxicity of mimulone was lower than somniferanolide and other compounds. Meanwhile, the most reported target of toxicity was the immunotoxicity shown by nine compounds (except mimulone and aurantinidin). Overall, ADMET results exhibited that all tested compounds possessed the drug-likeness properties. However, some compounds such as limonin, withanolide, tomentin A and aurantinidin showed more ideal ADME properties, while the mimulone exhibited lower toxicity potential.

Table 6

The ADMET results of selected phytochemicals

Compounds	Mol Wt[a]	TPSA[b]	HBD	HBA	log P	log S[c]	Caco2[d]	log BB	Rot	Acute tox.[e]	pLD_{50}[f]	Ames
Silymarin	482.441	155.14	5	10	2.3627	-3.204	0.435	-1.207	4	IV	2000	No
Limonin	470.518	104.57	0	8	3.1374	-4.379	0.952	-0.841	1	III	244	No
Withanolide	470.606	96.36	2	6	3.4954	-5.127	0.831	-0.315	2	III	300	No
Withasomnilide	470.606	96.36	2	6	3.4954	-5.209	0.834	0.022	2	II	7	No
(18R)-withaphysalin F	484.589	105.59	2	7	2.8318	-4.973	0.812	-0.422	1	II	7	No
Mimulone	408.494	86.99	3	5	5.7451	-3.817	0.651	-1.034	6	IV	2000	No
Silibinin	482.441	155.14	5	10	2.3627	-3.204	0.435	-1.207	4	IV	2000	No
Tomentin A	442.508	116.45	4	7	4.5348	-3.502	-0.366	-1.388	5	IV	2000	No
3-HDH-withanolide F	488.621	124.29	4	7	2.738	-5.209	0.668	-0.9	2	II	34	No
Somniferanolide	468.59	96.36	2	6	3.4155	-5.108	0.897	-0.347	2	II	34	No
Aurantinidin	287.247	114.29	5	6	2.9089	-2.968	-0.881	-1.612	1	V	3919	No

[a] Molecular weight in g/mol

[b] Topological polar surface area in Å²

[c] Aqueous solubility in log mol/L

[d] Predicted apparent Caco-2 cell permeability in 10^{-6} cm/s

[e] Acute toxicity according to the globally harmonized system (GHS) of classification and labeling of Chemicals

[f] Predicted LD_{50} in mg/kg

Molecular dynamics simulation

The best-docked pose with the highest binding affinity was utilized as the starting structure for the 100 ns Molecular dynamics simulation run. The best pose output is employed to build up this method in a high-throughput manner for studying the binding mechanism of the complex (ligand-protein) under clearly defined water environments. The different structures represented in Fig. 9 (a,b) give a visual impression of the sequence of events and the dynamics of the process, during the 1, 10, 20, 50, and 100 ns

MD simulation runs. To examine structural stability, MD data is processed by calculating the RMSD. Complexes of 1O86 and 6LU7 with withanolide formed stable conformation after ~60 ns and ~85 ns, respectively, with an appropriate RMSD value of 2.65 and 2.91 Å, respectively, as seen in the RMSD plot (Fig. 10). The most acceptable RMSD value range is < 3.0 Å, as the lower RMSD value indicates superior stability of the system [102]. This finding shows that the withanolide develop a stable protein-ligand combination. The drop in the RMSD value of protein-ligand complexes reflects a conformational alteration in the protein secondary structure due to ligand binding. To examine the average flexibility and fluctuation of individual amino acids, the RMSF of protein and complexes was plotted from a 100 ns MD trajectory (Fig 11). Several times during the ligand-bound state, the fluctuations of the residues in the protein could be found in the RMSF plot. The average RMSF values of 1.481 and 1.936 Å was observed for complexes 1O86-withanolide and 6LU7-withanolide, respectively. The findings show that ligand-protein interaction brings protein chains closer and reduces the gap between them, represented in Fig 12. For evaluating and comparing protein structures, RR distance maps represent the average distance and standard deviation for all amino acid pairings between two conformations. The RR distance maps are represented in Fig. 13, which plots patterns of spatial interaction [103, 104]. The white diagonal on the map shows the zero distance between two residues, while the red and blue elements represent residue pairings with the greatest distance variances in the two conformations. The lowest radius of gyration (Rg) value of ~23.47 and ~21.04 Å was observed for 1O86-withanolide and 6LU7-withanolide complexes, respectively. Along the simulation time, Rg for the protein-ligand combination decreased, indicating that the structure became more compact (Fig. 14).

Grid-search on 17x19x18 and 14x18x16 grids, rcut = 0.35 for 1O86 and 6LU7, respectively, revealed the interactions of ligand with protein *via* hydrogen bonds, which were plotted against time (Fig. 15). On calculating hydrogen bonds between ligand (36 atoms) and proteins (6007 and 3038 atoms for receptors 1O86 and 6LU7, respectively), 835 donors and 1663 acceptors were found for 1O86-withanolide complex, while 435 donors and 853 acceptors were found for the 6LU7-withanolide complex. The average number of hydrogen bonds per timeframe was observed to be 0.662 and 0.775 out of 694302 and 185528 possible for 1O86-withanolide and 6LU7-withanolide complexes, respectively. It can conclude that the interactions between ligand-protein substantially enhanced the number of H-bonds. Fig. 16 shows the solvent accessible surface area (SASA) values changed due to the binding of the ligand to the protein. The reduced value of SASA of protein upon binding to ligand indicates the alteration of conformation in the protein structure and reduction in pocket size with increased hydrophobicity around it.

Conclusion

In conclusion, our study exhibited that several phytochemicals are accomplished for inhibition of various targets of COVID-19. Among them, withanolide, (18R)-withaphysalin F, limonin and mimulone were active against the multiple targets. Furthermore, compounds such as limonin, withanolide, tomentin A, aurantinidine, and mimulone showed more ideal ADMET properties among the compounds with the best docking results. Molecular dynamic simulation of 100 ns run revealed that both the protein-ligand complexes possess stable conformation but protein1O86 forms a slightly more stable complex with withanolide than protein 6LU7. Our findings in this study could be a good starting point for carting out more *in vitro* and clinical studies to obtain potential drug candidates for the treatment of COVID-19 in the future.

Declarations

Funding:

The authors wish to thank Universiti Teknologi Malaysia and the Ministry of Higher Education (MOHE) Malaysia for funding this research under the Fundamental Research Grant Scheme (FRGS/1/2019/STG01/ UTM/02/7).

Conflict of Interest:

The authors have no conflict of interest to declare.

Availability of data and material:

All data and material generated or analyzed during this study are included in the article and supplementary materials.

Code availability:

Not applicable

Authors contributions:

Joazaizulfazli Jamalis, Sankaranarayanan Murugesan and Subhash Chander: supervision, investigation and critical review; Sonam Shakya, Harsha Kharkwal and Mohammad Rizki Fadhil Pratama: methodology, software's, investigation, formal analysis, data curation; Aso Hameed Hasan and Narmin Hama Amin Hussen: design of study, methodology, and writing-original draft.

References

1. Shahhosseini, N., et al., *Mutation Signatures and In Silico Docking of Novel SARS-CoV-2 Variants of Concern.* Microorganisms, 2021. **9**(5): p. 926.
2. Rezaei, M., et al., *ACE2: Its potential role and regulation in severe acute respiratory syndrome and COVID-19.* Journal of Cellular Physiology, 2021. **236**(4): p. 2430-2442.
3. Zaib, S., et al., *Machine Intelligence Techniques for the Identification and Diagnosis of COVID-19.* Current Medicinal Chemistry, 2021. **28**(26): p. 5268-5283.
4. WHO. *Coronavirus disease 2019 (COVID-19)*. 2021; Available from: https://covid19.who.int/.
5. *https://www.covid19treatmentguidelines.nih.gov/about-the-guidelines/whats-new/*.
6. Rehman, M., et al., *Therapeutic and vaccine strategies against SARS-CoV-2: past, present and future.* Future Virology, 2020. **15**(7): p. 471-482.
7. Chen, J. and H. Lu, *New challenges to fighting COVID-19: Virus variants, potential vaccines, and development of antivirals.* Biosci Trends, 2021. **15**(2): p. 126-128.
8. Andrei, G., *Vaccines and Antivirals: Grand Challenges and Great Opportunities.* Frontiers in Virology, 2021. **1**(8).
9. Anju, A., et al., *Virtual screening of quinoline derived library for SARS-COV-2 targeting viral entry and replication.* Journal of Biomolecular Structure and Dynamics, 2021: p. 1-30.
10. *Coronavirus (COVID-19) Vaccinations*. 2021; Available from: https://ourworldindata.org/covid-vaccinations.
11. *https://www.covid19treatmentguidelines.nih.gov/therapies/*.
12. Griffin, S., *Covid-19: Fully vaccinated people can carry as much delta virus as unvaccinated people, data indicate.* Bmj, 2021. **374**: p. n2074.
13. Kashte, S., et al., *COVID-19 vaccines: rapid development, implications, challenges and future prospects.* Human Cell, 2021. **34**(3): p. 711-733.
14. Antonelli, M., et al., *Risk factors and disease profile of post-vaccination SARS-CoV-2 infection in UK users of the COVID Symptom Study app: a prospective, community-based, nested, case-control study.* The Lancet Infectious Diseases, 2021.
15. Swan, D.A., et al., *COVID-19 vaccines that reduce symptoms but do not block infection need higher coverage and faster rollout to achieve population impact.* Scientific Reports, 2021. **11**(1): p. 15531.
16. Pavia, C.S. and G.P. Wormser, *Passive immunization and its rebirth in the era of the COVID-19 pandemic.* International Journal of Antimicrobial Agents, 2021. **57**(3): p. 106275.
17. Skariyachan, S., et al., *Structural and molecular basis of the interaction mechanism of selected drugs towards multiple targets of SARS-CoV-2 by molecular docking and dynamic simulation studies- deciphering the scope of repurposed drugs.* Computers in Biology and Medicine, 2020. **126**: p. 104054.
18. Ledford, H., *Covid antiviral pills: what scientists still want to know.* Nature, 2021. **599**(7885): p. 358-359.
19. Awadasseid, A., et al., *Effective drugs used to combat SARS-CoV-2 infection and the current status of vaccines.* Biomedicine & Pharmacotherapy, 2021. **137**: p. 111330.
20. Poduri, R., G. Joshi, and G. Jagadeesh, *Drugs targeting various stages of the SARS-CoV-2 life cycle: Exploring promising drugs for the treatment of Covid-19.* Cellular Signalling, 2020. **74**: p. 109721.
21. Fakhri, S., et al., *Targeting Multiple Signal Transduction Pathways of SARS-CoV-2: Approaches to COVID-19 Therapeutic Candidates.* Molecules, 2021. **26**(10): p. 2917.

22. Elhady, S.S., et al., *Molecular Docking and Dynamics Simulation Study of Hyrtioserectus Isolated Scalarane Sesterterpenes as Potential SARS-CoV-2 Dual Target Inhibitors.* Biology, 2021. **10**(5): p. 389.
23. Su, H., Y. Xu, and H. Jiang, *Drug discovery and development targeting the life cycle of SARS-CoV-2.* Fundamental Research, 2021. **1**(2): p. 151-165.
24. Zhang, H. and H. Zhang, *Entry, egress and vertical transmission of SARS-CoV-2.* J Mol Cell Biol, 2021. **13**(3): p. 168-174.
25. Hu, X., et al., *Discovery of TMPRSS2 Inhibitors from Virtual Screening as a Potential Treatment of COVID-19.* ACS Pharmacology & Translational Science, 2021. **4**(3): p. 1124-1135.
26. Hoffmann, M., et al., *SARS-CoV-2 Cell Entry Depends on ACE2 and TMPRSS2 and Is Blocked by a Clinically Proven Protease Inhibitor.* Cell, 2020. **181**(2): p. 271-280.e8.
27. Vincent, M.J., et al., *Chloroquine is a potent inhibitor of SARS coronavirus infection and spread.* Virology Journal, 2005. **2**(1): p. 69.
28. Ren, L., et al., *Assessment of Chloroquine and Hydroxychloroquine Safety Profiles: A Systematic Review and Meta-Analysis.* Frontiers in Pharmacology, 2020. **11**(1584).
29. Yamamoto, M., et al., *Identification of Nafamostat as a Potent Inhibitor of Middle East Respiratory Syndrome Coronavirus S Protein-Mediated Membrane Fusion Using the Split-Protein-Based Cell-Cell Fusion Assay.* Antimicrobial Agents and Chemotherapy, 2016. **60**(11): p. 6532-6539.
30. Trougakos, I.P., et al., *Insights to SARS-CoV-2 life cycle, pathophysiology, and rationalized treatments that target COVID-19 clinical complications.* Journal of Biomedical Science, 2021. **28**(1): p. 9.
31. Tang, T., et al., *Coronavirus membrane fusion mechanism offers a potential target for antiviral development.* Antiviral Research, 2020. **178**: p. 104792.
32. Faheem, et al., *Druggable targets of SARS-CoV-2 and treatment opportunities for COVID-19.* Bioorganic Chemistry, 2020. **104**: p. 104269.
33. Kishk, S.M., et al., *Molecular Insights into Human Transmembrane Protease Serine-2 (TMPS2) Inhibitors against SARS-CoV2: Homology Modelling, Molecular Dynamics, and Docking Studies.* Molecules, 2020. **25**(21): p. 5007.
34. Sola, I., et al., *Continuous and Discontinuous RNA Synthesis in Coronaviruses.* Annual Review of Virology, 2015. **2**(1): p. 265-288.
35. V'kovski, P., et al., *Coronavirus biology and replication: implications for SARS-CoV-2.* Nature Reviews Microbiology, 2021. **19**(3): p. 155-170.
36. Wu, C., et al., *Analysis of therapeutic targets for SARS-CoV-2 and discovery of potential drugs by computational methods.* Acta Pharmaceutica Sinica B, 2020. **10**(5): p. 766-788.
37. Marinho, E.M., et al., *Virtual screening based on molecular docking of possible inhibitors of Covid-19 main protease.* Microbial Pathogenesis, 2020. **148**: p. 104365.
38. Huseen, N.H.A., *Docking study of naringin binding with COVID-19 main protease enzyme.* Iraqi Journal of Pharmaceutical Sciences (P-ISSN: 1683-3597, E-ISSN: 2521-3512), 2020. **29**(2): p. 231-238.
39. Gao, X., et al., *Crystal structure of SARS-CoV-2 papain-like protease.* Acta Pharmaceutica Sinica B, 2021. **11**(1): p. 237-245.
40. Li, X., et al., *Possible Targets of Pan-Coronavirus Antiviral Strategies for Emerging or Re-Emerging Coronaviruses.* Microorganisms, 2021. **9**(7): p. 1479.
41. Abu-Melha, S., et al., *Clean Grinding Technique: A Facile Synthesis and In Silico Antiviral Activity of Hydrazones, Pyrazoles, and Pyrazines Bearing Thiazole Moiety against SARS-CoV-2 Main Protease (Mpro).* Molecules, 2020. **25**(19): p. 4565.
42. Kong, R., et al., *COVID-19 Docking Server: a meta server for docking small molecules, peptides and antibodies against potential targets of COVID-19.* Bioinformatics, 2020. **36**(20): p. 5109-5111.
43. Tang, B., et al., *AI-aided design of novel targeted covalent inhibitors against SARS-CoV-2.* bioRxiv, 2020: p. 2020.03.03.972133.
44. Banerjee, R., L. Perera, and L.M.V. Tillekeratne, *Potential SARS-CoV-2 main protease inhibitors.* Drug Discovery Today, 2021. **26**(3): p. 804-816.
45. Vandyck, K. and J. Deval, *Considerations for the discovery and development of 3-chymotrypsin-like cysteine protease inhibitors targeting SARS-CoV-2 infection.* Current Opinion in Virology, 2021. **49**: p. 36-40.
46. Dong, L., S. Hu, and J. Gao, *Discovering drugs to treat coronavirus disease 2019 (COVID-19).* Drug Discov Ther, 2020. **14**(1): p. 58-60.

47. Cao, B., et al., *A Trial of Lopinavir-Ritonavir in Adults Hospitalized with Severe Covid-19.* N Engl J Med, 2020. **382**(19): p. 1787-1799.
48. Anirudhan, V., et al., *Targeting SARS-CoV-2 viral proteases as a therapeutic strategy to treat COVID-19.* J Med Virol, 2021. **93**(5): p. 2722-2734.
49. Lin, M.-H., et al., *Disulfiram can inhibit MERS and SARS coronavirus papain-like proteases via different modes.* Antiviral Research, 2018. **150**: p. 155-163.
50. Yin, W., et al., *Structural basis for inhibition of the RNA-dependent RNA polymerase from SARS-CoV-2 by remdesivir.* Science, 2020. **368**(6498): p. 1499-1504.
51. de Wit, E., et al., *Prophylactic and therapeutic remdesivir (GS-5734) treatment in the rhesus macaque model of MERS-CoV infection.* Proceedings of the National Academy of Sciences, 2020. **117**(12): p. 6771-6776.
52. Sheahan, T.P., et al., *Comparative therapeutic efficacy of remdesivir and combination lopinavir, ritonavir, and interferon beta against MERS-CoV.* Nature Communications, 2020. **11**(1): p. 222.
53. Wang, M., et al., *Remdesivir and chloroquine effectively inhibit the recently emerged novel coronavirus (2019-nCoV) in vitro.* Cell Research, 2020. **30**(3): p. 269-271.
54. Singh, T.U., et al., *Drug repurposing approach to fight COVID-19.* Pharmacological Reports, 2020. **72**(6): p. 1479-1508.
55. Malone, B. and E.A. Campbell, *Molnupiravir: Coding for catastrophe.* Nature Structural & Molecular Biology, 2021. **28**(9): p. 706-708.
56. Naveed, M., et al., *Design of a novel multiple epitope-based vaccine: An immunoinformatics approach to combat SARS-CoV-2 strains.* Journal of Infection and Public Health, 2021. **14**(7): p. 938-946.
57. *https://www.who.int/news/item/28-11-2021-update-on-omicron*.
58. Vardhan, S. and S.K. Sahoo, *In silico ADMET and molecular docking study on searching potential inhibitors from limonoids and triterpenoids for COVID-19.* Computers in Biology and Medicine, 2020. **124**: p. 103936.
59. Vijesh, A.M., et al., *Molecular docking studies of some new imidazole derivatives for antimicrobial properties.* Arabian Journal of Chemistry, 2013. **6**(2): p. 197-204.
60. Alfarisi, S., et al., *Synthesis, Antimicrobial Study, and Molecular Docking Simulation of 3,4-Dimethoxy-β-Nitrostyrene Derivatives as Candidate PTP1B Inhibitor.* Scientia Pharmaceutica, 2020. **88**(3): p. 37.
61. Abu-Melha, S., et al., *Potential COVID-19 Drug Candidates Based on Diazinyl-Thiazol-Imine Moieties: Synthesis and Greener Pastures Biological Study.* Molecules, 2022. **27**(2): p. 488.
62. Jain, R. and S. Mujwar, *Repurposing metocurine as main protease inhibitor to develop novel antiviral therapy for COVID-19.* Structural Chemistry, 2020. **31**(6): p. 2487-2499.
63. Yang, Y., et al., *Traditional Chinese Medicine in the Treatment of Patients Infected with 2019-New Coronavirus (SARS-CoV-2): A Review and Perspective.* International journal of biological sciences, 2020. **16**(10): p. 1708-1717.
64. Liu, M., et al., *Efficacy and Safety of Integrated Traditional Chinese and Western Medicine for Corona Virus Disease 2019 (COVID-19): a systematic review and meta-analysis.* Pharmacological research, 2020. **158**: p. 104896-104896.
65. Ho, L.T.F., et al., *Highlights of traditional Chinese medicine frontline expert advice in the China national guideline for COVID-19.* Eur J Integr Med, 2020. **36**: p. 101116.
66. Anand, A.V., et al., *Medicinal Plants, Phytochemicals, and Herbs to Combat Viral Pathogens Including SARS-CoV-2.* Molecules, 2021. **26**(6): p. 1775.
67. Fakhri, S., et al., *Targeting Neurological Manifestations of Coronaviruses by Candidate Phytochemicals: A Mechanistic Approach.* Front Pharmacol, 2020. **11**: p. 621099.
68. Parida, P.K., D. Paul, and D. Chakravorty, *Nature's therapy for COVID-19: Targeting the vital non-structural proteins (NSP) from SARS-CoV-2 with phytochemicals from Indian medicinal plants.* Phytomedicine Plus, 2021. **1**(1): p. 100002.
69. Lalani, S. and C.L. Poh, *Flavonoids as Antiviral Agents for Enterovirus A71 (EV-A71).* Viruses, 2020. **12**(2).
70. Khan, S.L., et al., *Discovery of Potential Inhibitors of SARS-CoV-2 (COVID-19) Main Protease (M^{pro}) from Nigella Sativa (Black Seed) by Molecular Docking Study.* Coronaviruses, 2021. **2**(3): p. 384-402.
71. Ben-Shabat, S., et al., *Antiviral effect of phytochemicals from medicinal plants: Applications and drug delivery strategies.* Drug Delivery and Translational Research, 2020. **10**(2): p. 354-367.

72. Kim, C.-H., *Anti–SARS-CoV-2 Natural Products as Potentially Therapeutic Agents.* Frontiers in Pharmacology, 2021. **12**(1015).
73. Fielding, B.C., et al., *Alkaloids: Therapeutic Potential against Human Coronaviruses.* Molecules, 2020. **25**(23).
74. Diniz, L.R.L., et al., *Bioactive Terpenes and Their Derivatives as Potential SARS-CoV-2 Proteases Inhibitors from Molecular Modeling Studies.* Biomolecules, 2021. **11**(1): p. 74.
75. Abdelmohsen, U.R., et al., *Natural coumarins as potential anti-SARS-CoV-2 agents supported by docking analysis.* RSC Advances, 2021. **11**(28): p. 16970-16979.
76. Wahedi, H.M., S. Ahmad, and S.W. Abbasi, *Stilbene-based natural compounds as promising drug candidates against COVID-19.* Journal of Biomolecular Structure and Dynamics, 2021. **39**(9): p. 3225-3234.
77. Xu, X.-Y., et al., *Plant-derived lignans as potential antiviral agents: a systematic review.* Phytochemistry Reviews, 2021.
78. Pandey, P., et al., *Targeting SARS-CoV-2 spike protein of COVID-19 with naturally occurring phytochemicals: an in silico study for drug development.* Journal of Biomolecular Structure and Dynamics, 2021. **39**(16): p. 6306-6316.
79. Daoui, O., et al., *3D-QSAR, ADME-Tox, and molecular docking of semisynthetic triterpene derivatives as antibacterial and insecticide agents.* Structural Chemistry, 2022.
80. Akdemir, A., et al., *Novel 2-indolinones containing a sulfonamide moiety as selective inhibitors of candida β-carbonic anhydrase enzyme.* Journal of enzyme inhibition and medicinal chemistry, 2019. **34**(1): p. 528-531.
81. Biovia, D., et al. *Dassault systèmes BIOVIA, discovery studio visualizer, v. 17.2, San Diego: Dassault Systèmes, 2016.* J. Chem. Phys 2000 [cited 10; 21-9991].
82. Morris, G.M., et al., *Automated docking using a Lamarckian genetic algorithm and an empirical binding free energy function.* Journal of Computational Chemistry, 1998. **19**(14): p. 1639-1662.
83. Trott, O. and A.J. Olson, *AutoDock Vina: improving the speed and accuracy of docking with a new scoring function, efficient optimization, and multithreading.* Journal of computational chemistry, 2010. **31**(2): p. 455-461.
84. Pratama, M.R.F., H. Poerwono, and S. Siswodiharjo, *ADMET properties of novel 5-O-benzoylpinostrobin derivatives.* Journal of Basic and Clinical Physiology and Pharmacology, 2019. **30**(6).
85. Vanommeslaeghe, K., et al., *CHARMM general force field: A force field for drug-like molecules compatible with the CHARMM all-atom additive biological force fields.* Journal of Computational Chemistry, 2010. **31**(4): p. 671-690.
86. Yu, W., et al., *Extension of the CHARMM general force field to sulfonyl-containing compounds and its utility in biomolecular simulations.* Journal of Computational Chemistry, 2012. **33**(31): p. 2451-2468.
87. Jorgensen, W.L., et al., *Comparison of simple potential functions for simulating liquid water.* The Journal of Chemical Physics, 1983. **79**(2): p. 926-935.
88. Allen, M.P. and D.J. Tildesley, *Computer simulation of liquids*. 2017: Oxford university press.
89. Essmann, U., et al., *A smooth particle mesh Ewald method.* The Journal of chemical physics, 1995. **103**(19): p. 8577-8593.
90. Steinbach, P.J. and B.R. Brooks, *New spherical-cutoff methods for long-range forces in macromolecular simulation.* Journal of Computational Chemistry, 1994. **15**(7): p. 667-683.
91. Humphrey, W., A. Dalke, and K. Schulten, *VMD: Visual molecular dynamics.* Journal of Molecular Graphics, 1996. **14**(1): p. 33-38.
92. DeLano, W.L., *Pymol: An open-source molecular graphics tool.* CCP4 Newsletter on protein crystallography, 2002. **40**(1): p. 82-92.
93. Su, X., et al., *Biological fingerprinting analysis of traditional Chinese medicines with targeting ADME/Tox property for screening of bioactive compounds by chromatographic and MS methods.* Mini Rev Med Chem, 2007. **7**(1): p. 87-98.
94. Gil, C., et al., *COVID-19: Drug Targets and Potential Treatments.* Journal of medicinal chemistry, 2020. **63**(21): p. 12359-12386.
95. Das, G., et al., *An overview of key potential therapeutic strategies for combat in the COVID-19 battle.* RSC Advances, 2020. **10**(47): p. 28243-28266.
96. Liu, C., et al., *Research and Development on Therapeutic Agents and Vaccines for COVID-19 and Related Human Coronavirus Diseases.* ACS Central Science, 2020. **6**(3): p. 315-331.
97. Hasan, A.H., et al., *Novel thiophene Chalcones-Coumarin as acetylcholinesterase inhibitors: Design, synthesis, biological evaluation, molecular docking, ADMET prediction and molecular dynamics simulation.* Bioorganic Chemistry, 2022. **119**: p. 105572.

98. Prasanna, S. and J.R. Doerksen, *Topological Polar Surface Area: A Useful Descriptor in 2D-QSAR.* Current Medicinal Chemistry, 2009. **16**(1): p. 21-41.
99. Banerjee, P., et al., *ProTox-II: a webserver for the prediction of toxicity of chemicals.* Nucleic Acids Research, 2018. **46**(W1): p. W257-W263.
100. Chander, S., et al., *Design, synthesis and in-vitro evaluation of novel tetrahydroquinoline carbamates as HIV-1 RT inhibitor and their antifungal activity.* Bioorganic Chemistry, 2016. **64**: p. 66-73.
101. Chander, S., et al., *Rational design, synthesis, anti-HIV-1 RT and antimicrobial activity of novel 3-(6-methoxy-3,4-dihydroquinolin-1(2H)-yl)-1-(piperazin-1-yl)propan-1-one derivatives.* Bioorganic Chemistry, 2016. **67**: p. 75-83.
102. Kufareva, I. and R. Abagyan, *Methods of protein structure comparison.* Methods in molecular biology (Clifton, N.J.), 2012. **857**: p. 231-257.
103. Wu, S. and Y. Zhang, *A comprehensive assessment of sequence-based and template-based methods for protein contact prediction.* Bioinformatics, 2008. **24**(7): p. 924-31.
104. Khan, M.D., et al., *Low concentrated phosphorus sorption in aqueous medium on aragonite synthesized by carbonation of seashells: Optimization, kinetics, and mechanism study.* Journal of Environmental Management, 2021. **280**: p. 111652.

Figures

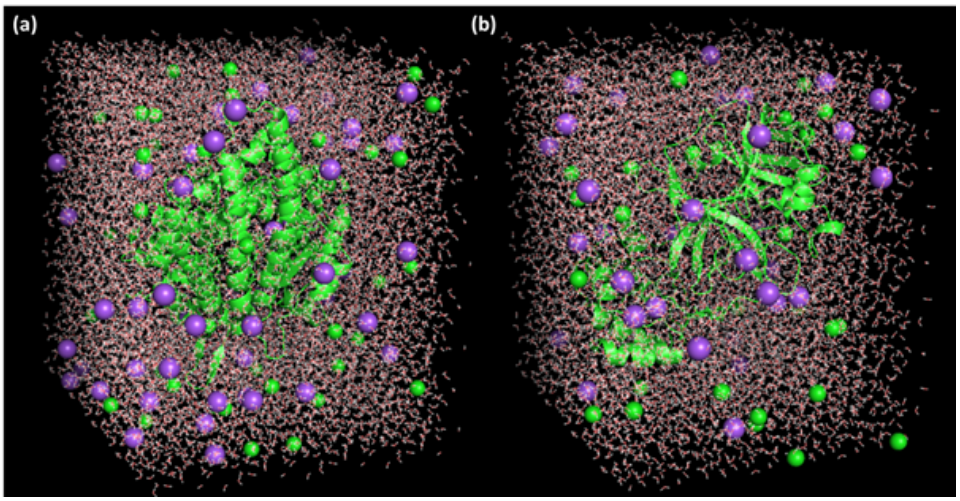


Figure 1

Protein-ligand complex of (a) protein 1O86 and (b) protein 6LU7 in triclinic box solvated with water molecules and neutralized with 55 Na^+ and 42 Cl^- ions, and 33 Na^+ and 29 Cl^- ions (0.15 M salt), respectively.

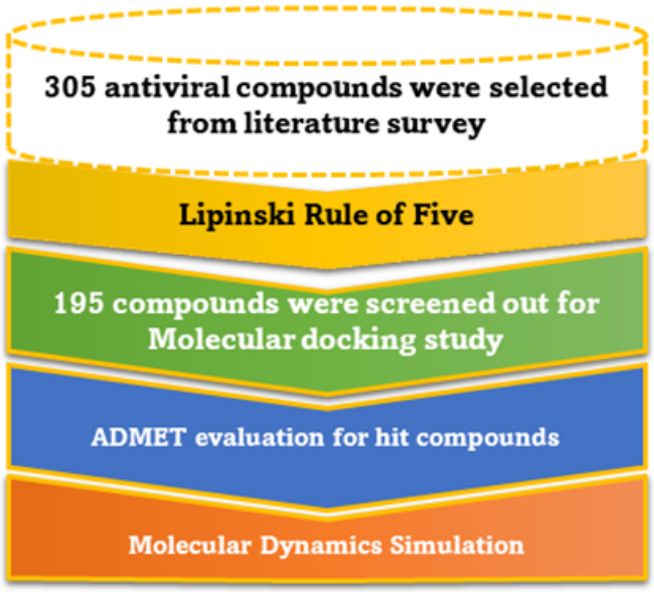


Figure 2

Overall workflow of the present study

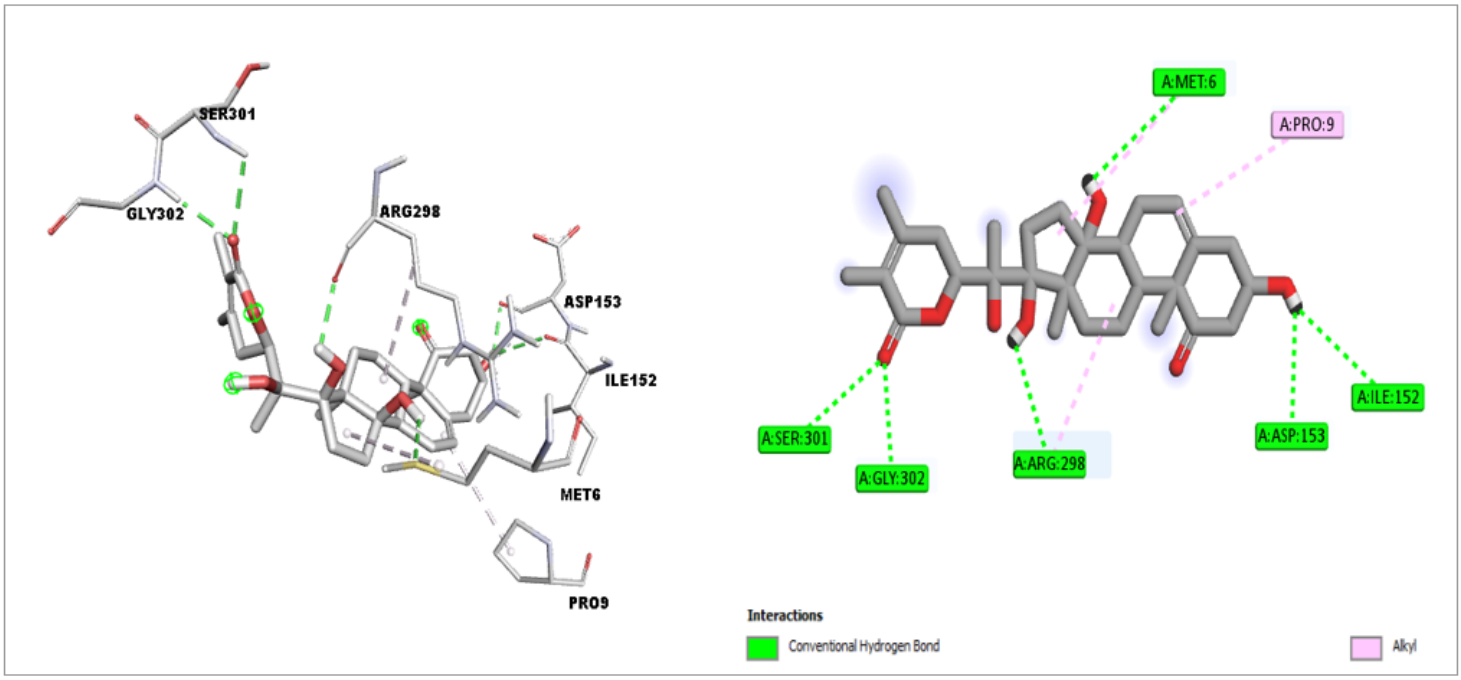


Figure 3

Molecular interactions of 3-HDH-withanolide F with COVID-19 M^{pro} residues (PDB ID: 6LU7)

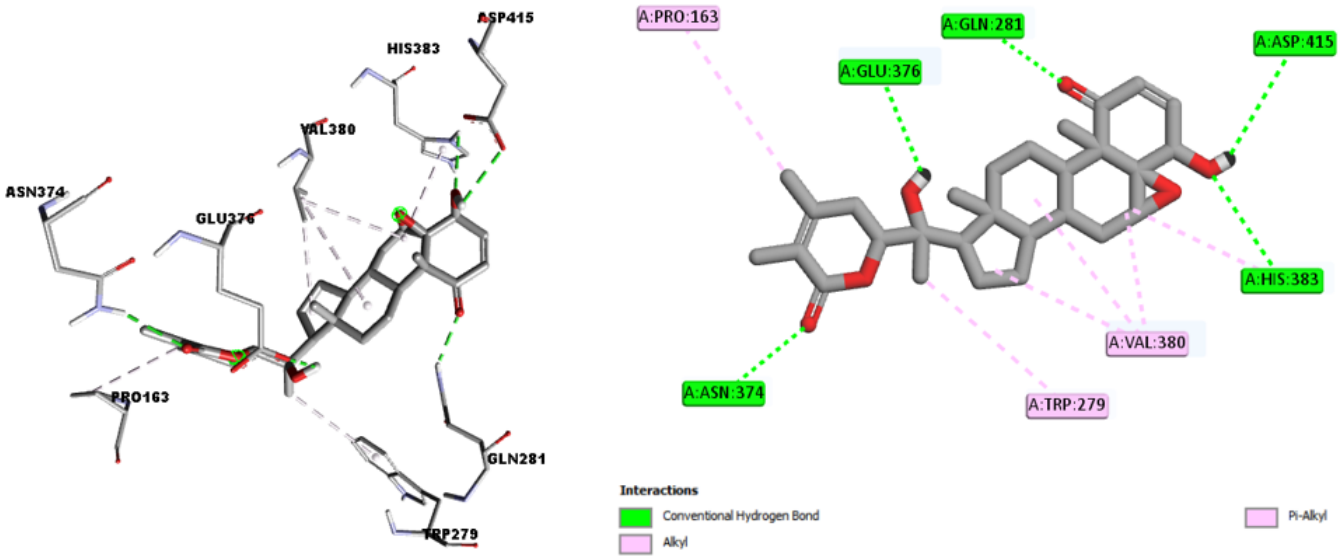


Figure 4

Molecular interactions of withanolide with COVID-19 ACE residues (PDB ID: 1O86)

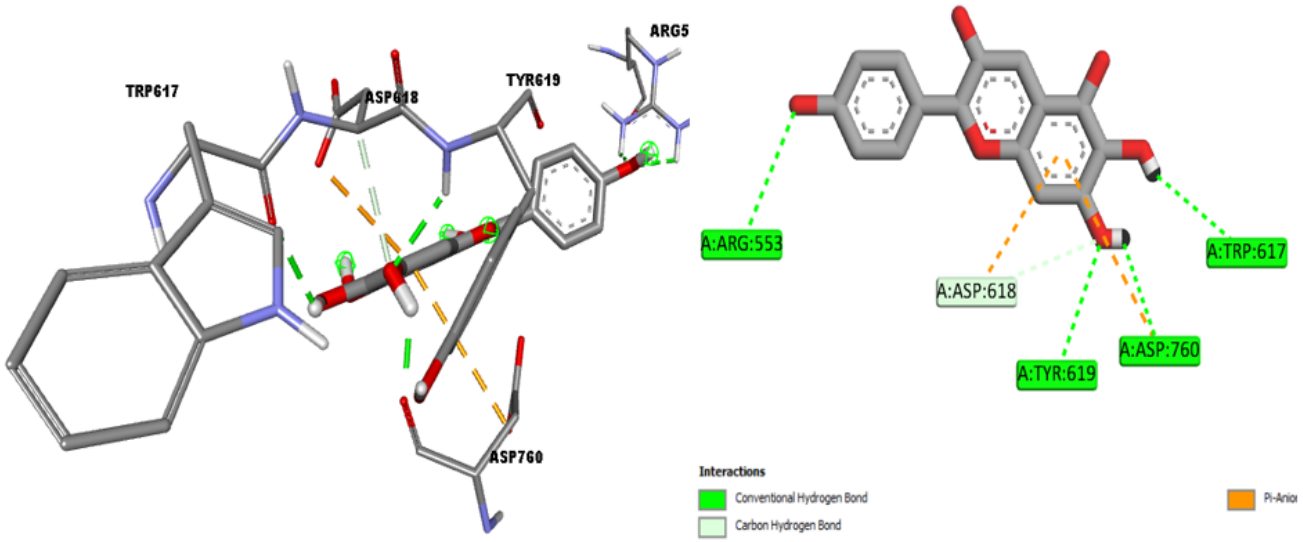


Figure 5

Molecular interactions of aurantinidin with COVID-19 RdRp residues (PDB ID: 7BV2)

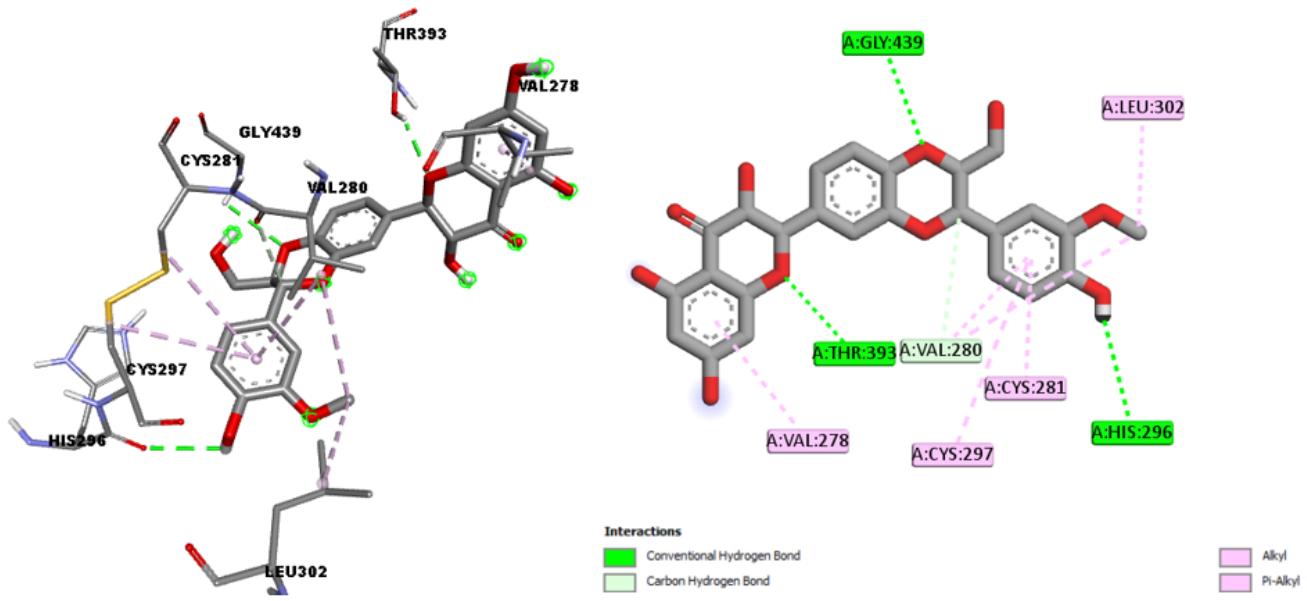


Figure 6

Molecular interactions of Silibinin with COVID-19 TMPRSS2 residues (PDB ID: 7MEQ)

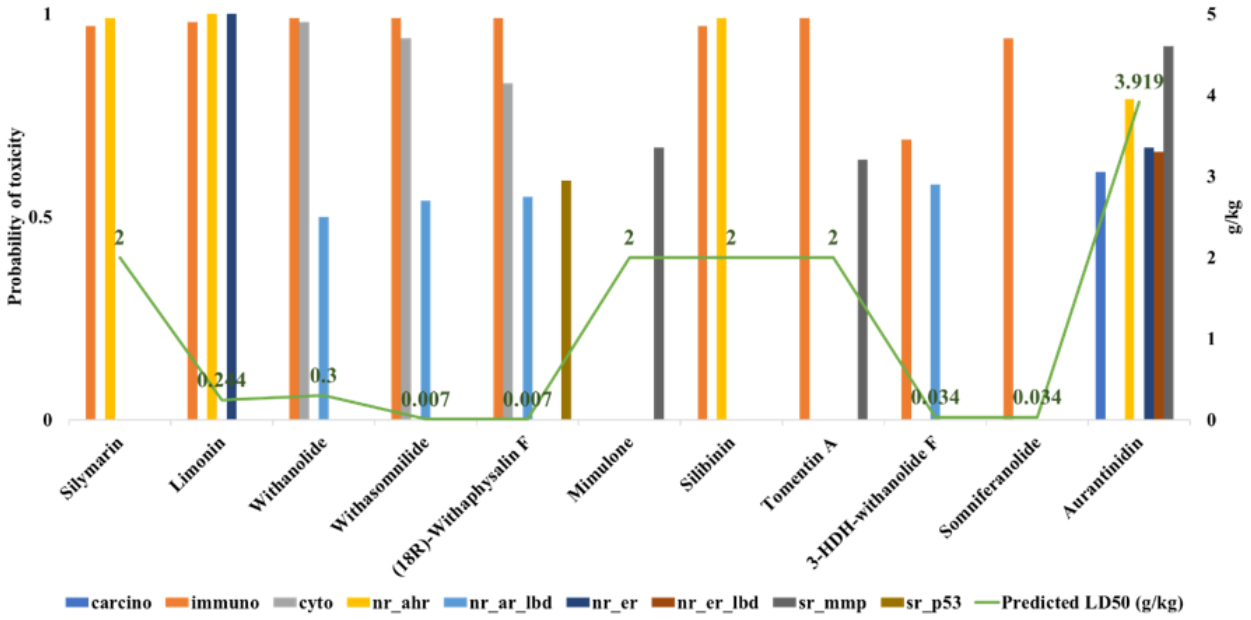


Figure 8

Predicted toxicity parameters with ProTox-II

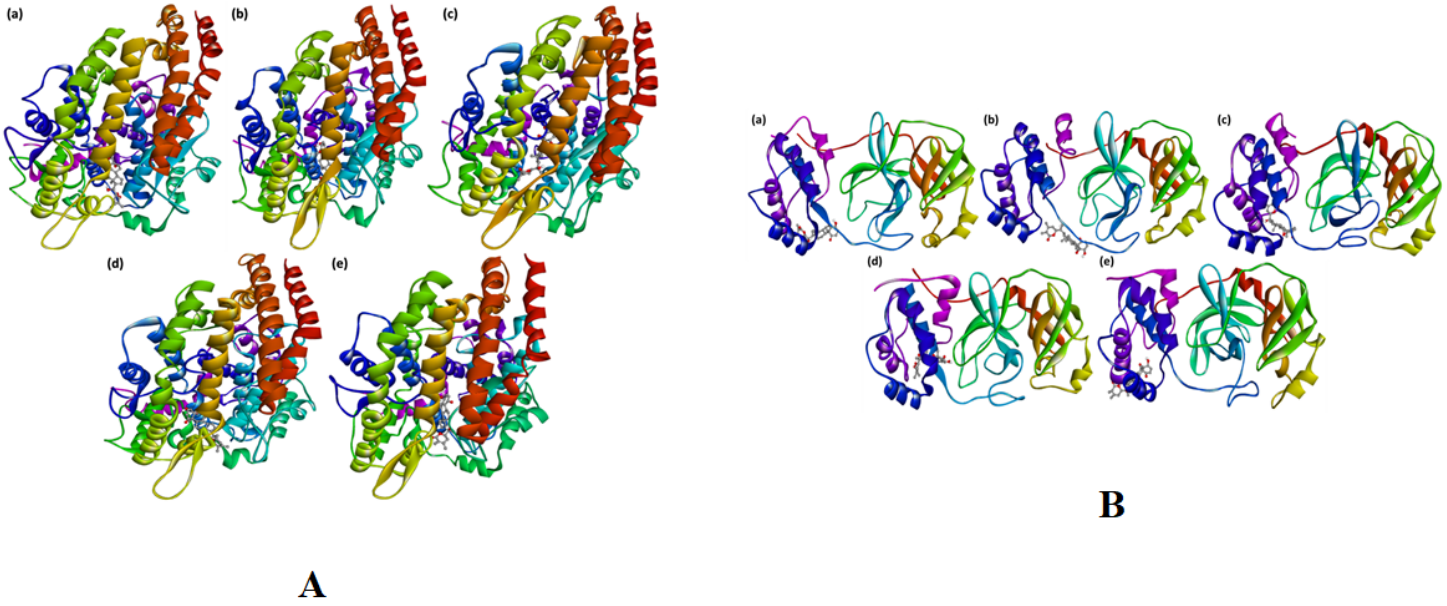


Figure 9

(a). Protein 1O86-withanolide structures at (a) 1 ns, (b) 10 ns, (c) 20 ns, (d) 50 ns, and (e) 100 ns MD run, giving a visual impression of the sequence of events and the dynamics of the process.

(b). Protein 6LU7-withanolide structures at (a) 1 ns, (b) 10 ns, (c) 20 ns, (d) 50 ns, and (e) 100 ns MD run, giving a visual impression of the sequence of events and the dynamics of the process.

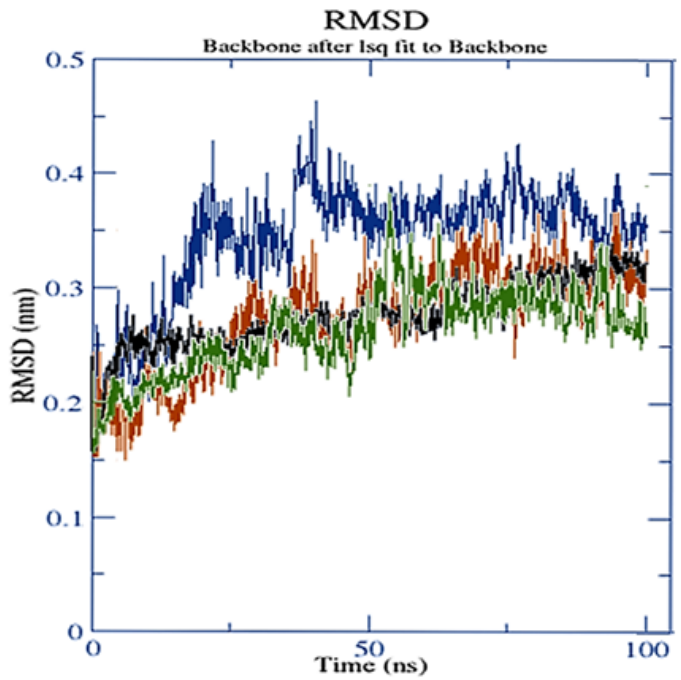


Figure 10

The RMSD of solvated protein backbone and complex during 100 ns MD simulation [protein 1O86-withanolide complex (green) and protein 6LU7-withanolide complex (brown)], and unbound protein 1O86 (black), unbound protein 6LU7 (blue).

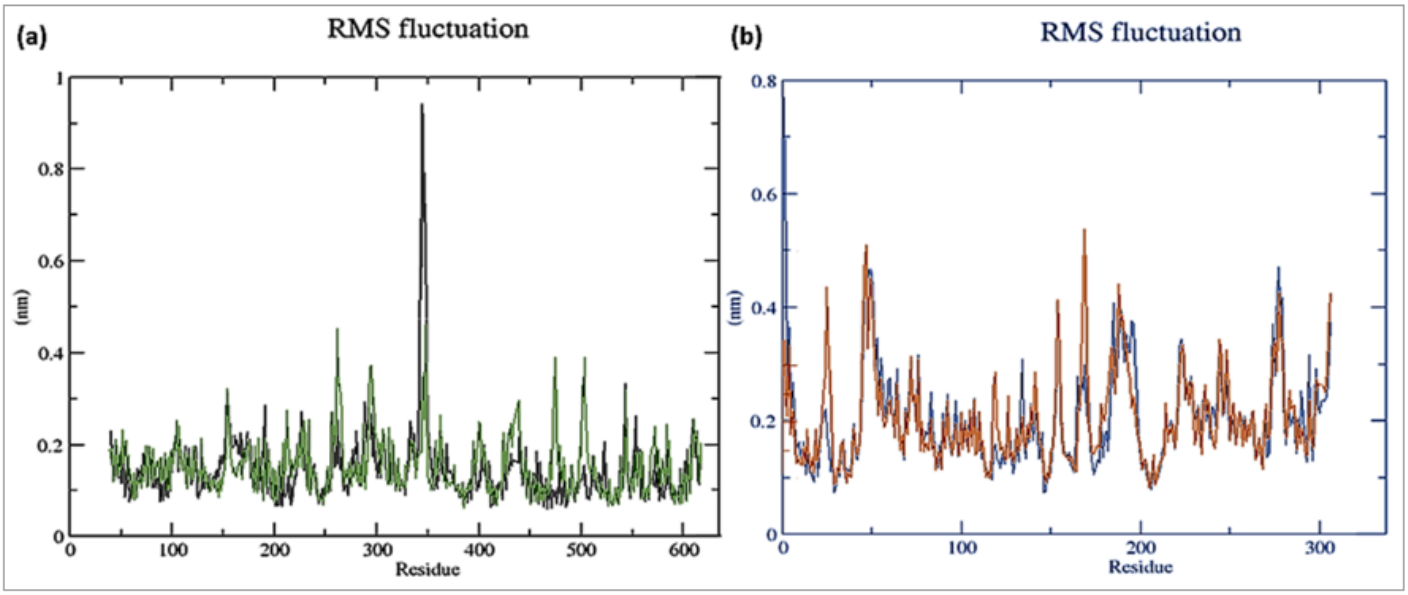


Figure 11

The RMSF values of solvated (a) unbound protein 1O86 (black), protein 1O86-withanolide complex (green), and (b) unbound protein 6LU7 (blue), protein 6LU7-withanolide complex (brown) plotted vs amino acid numbers.

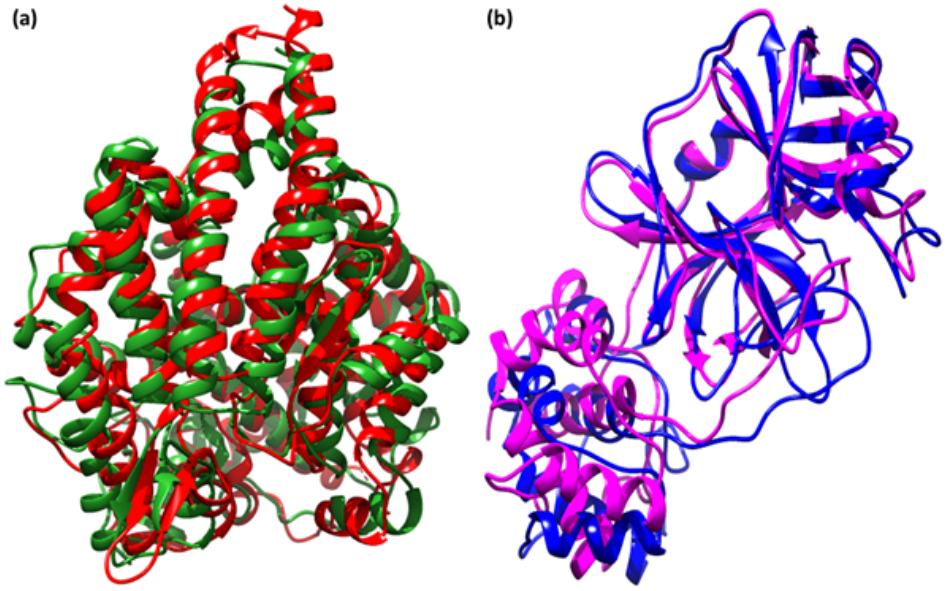


Figure 12

Superimposed structure of (a) unbounded protein1O86 (red) and protein1O86 after simulation (green) and (b) unbounded protein 6LU7 (blue) and protein 6LU7 after simulation (pink).

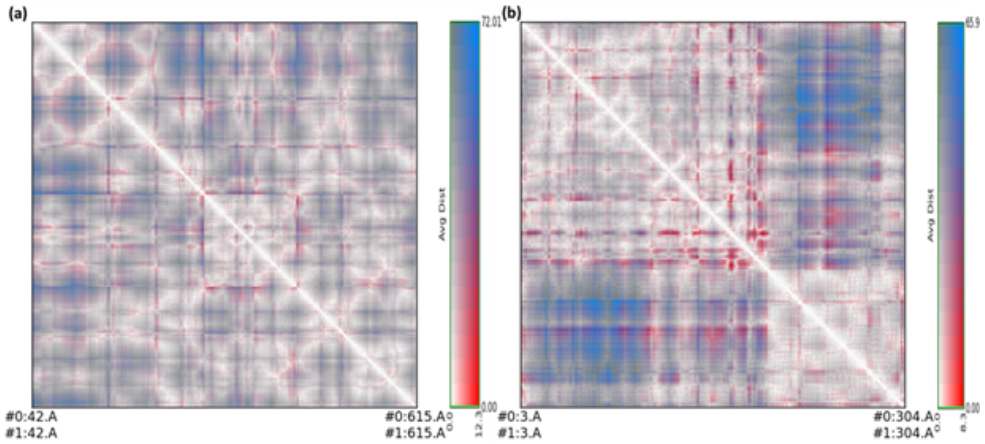


Figure 13

RR distance map displaying patterns of spatial interactions of proteins (a) 1O86 and (b) 6LU7, showing the average distance and standard deviation for all amino acid pairs.

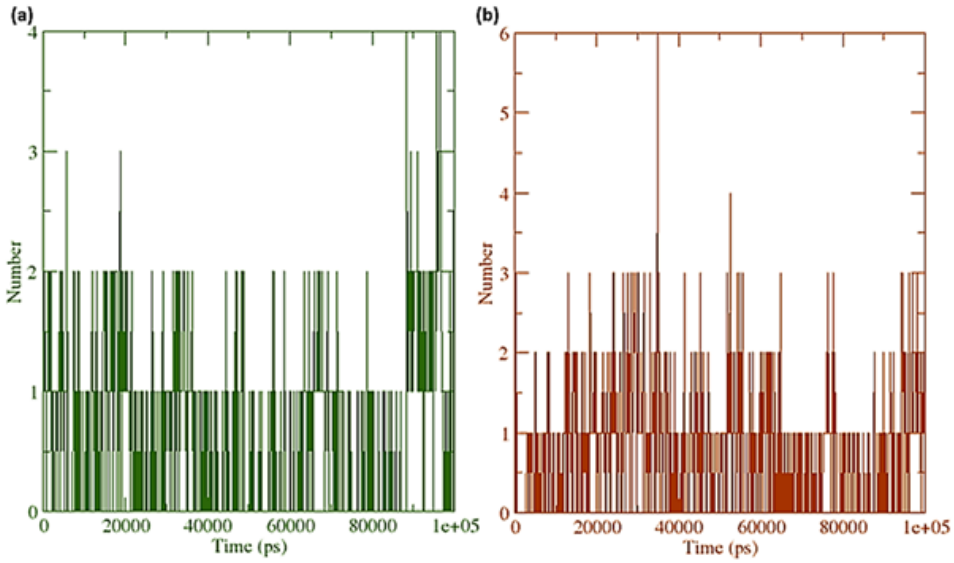


Figure 15

Number of average hydrogen bonding interactions between (a) 1O86-withanolide complex and (b) 6LU7-withanolide complex during 100 ns simulation.

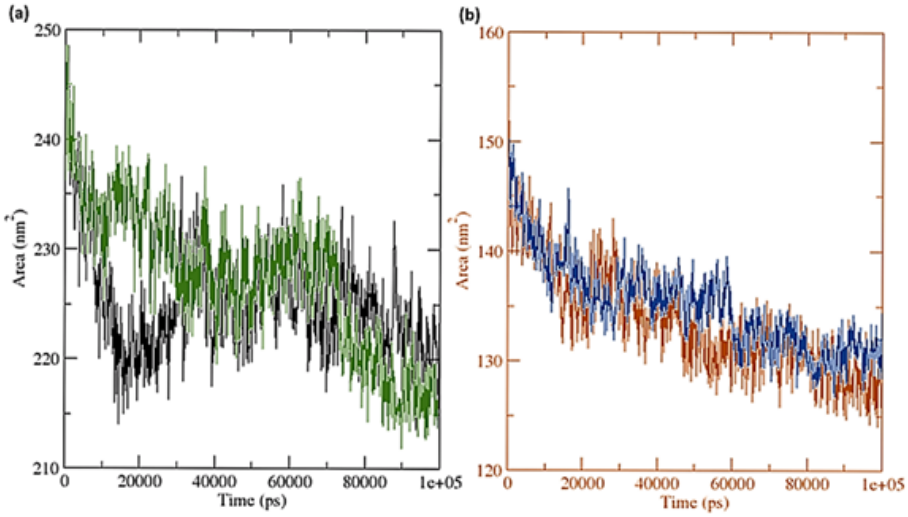


Figure 16

Solvent accessible surface area analysis for (a) unbound protein 1O86 (black), 1O86-withanolide complex (green), and (b) unbound protein 6LU7 (blue), 6LU7-withanolide complex (brown) during 100 ns simulation time.

Supplementary Files

This is a list of supplementary files associated with this preprint. Click to download.

- S1.docx